Progress In Electromagnetics Research Letters, Vol. 82, 9–16, 2019

Design of a Novel Multi-Layer Wideband Bandpass Filter with a Notched Band

Xiao-Chun Ji[1, 2], Wu-Sheng Ji[1, 2, *], Li-Ying Feng[1, 2],
Ying-Yun Tong[1, 2], and Zhi-Yue Zhang[1, 2]

Abstract—A wideband filter with a notched band is presented. The proposed filter is formed by cascading three coupling units, and each coupling unit is composed of two curved T-shaped microstrip patches at the top and bottom layers and a circular coupling slot at the mid layer. Overlapping three coupling units could result in a wideband filter with a tunable notched band. To analyse the resonance characteristics, the equivalent circuit model is presented. The notched frequency is 5.8 GHz, and within the passband, the insertion and return losses are better than −2 dB and −15 dB, respectively. The group delays are 0.08 ns and 0.12 ns correspondingly, and the upper stopband reaches 15 GHz. The multi-layer structure leads to a compact size and tight coupling characteristics, and the feasibility and excellent performance of the design is verified.

1. INTRODUCTION

With development of modern wireless systems, demands for wireless communication change from initial voice transmission to high-speed transmissions such as files, images, and multimedia. However, narrow-band communication systems could not satisfy those demands anymore, thus the research of broadband has been an inevitable trend. Wideband filters, especially ultra-wideband (UWB) filters [1], have been attracting more and more attention in industry and academia. Meanwhile, most of the WLAN systems are designed to operate in the 2.4 GHz (IEEE 802.11b and g) and 5.0 GHz frequency bands, e.g., 5.15 to 5.35 GHz (IEEE 802.11a lower bands) and 5.725 to 5.825 GHz (IEEE 802.11a upper bands) are used in the USA. For eliminating the interference of these WLAN radio signals in UWB services, the wideband filter with notched characteristic comes to be a requirement.

UWB [2, 3] and notched filters [4] with multiple-mode resonator (MMR) can generate multiple transmission poles in the band to enhance circuit coupling, while the high fabricated precision of 0.05 mm is hard to realize [2, 4]. Other filters with defected ground structure (DGS) [5, 6] and triangular ring loaded stub resonator (TRLSR) [7] have a very narrow notched band, but they are not suitable for eliminating all WLAN signals in 5–6 GHz.

[8] proposes a three-layer ultra-wideband coupler. There is a broadside coupling between the elliptical patches at the upper and bottom layers and the elliptical slots at the mid ground layer, and the coupling characteristics are analyzed. Based on this structure, [9, 10] propose a UWB filter. These designs have realized tight coupling and miniaturization, and the fabrication difficulties as in [2–4] are avoided simultaneously.

In this paper, a novel resonator is proposed by utilizing broadside coupling between the two curved T-shaped microstrip patches at the top and bottom layers and a circular coupling slot at the mid layer. Cascading three resonators could lead to UWB characteristics, as well as a notched band if those three

---

Received 11 December 2018, Accepted 23 January 2019, Scheduled 20 February 2019

[*] Corresponding author: Wu-Sheng Ji (jiwusheng@tute.edu.cn).

[1] Institute of Antenna and Microwave Techniques, Tianjin University of Technology and Education, Tianjin 300222, China. [2] School of Electronic Engineering, Tianjin University of Technology and Education, Tianjin 300222, China.

coupling units are close to each other to be partially overlapped. The equivalent circuit and methods to adjust the notched band are given, and consequently the characteristics of UWB and notched band have been analyzed. Finally, a prototype with notched band of 5.8 GHz is fabricated, validating an excellent circuit performance. Compared with [9, 10], the novel broadside coupling circuits could be used to design UWB devices, as well as a wideband filter with notched band which could eliminate all the WLAN signals within 5–6 GHz.

2. THE DESIGN OF FILTER

2.1. The Design of UWB Filter

The structure of the proposed filter is shown in Fig. 1. Fig. 1(a) depicts the 3-D view. The circuit consists of three coupling units, and each one includes two curved T-shaped microstrip patches at the top and bottom microstrip layers and a circular coupling slot at the mid ground layer. The curved T-shaped microstrip patch is composed of a large semicircle with diameter of D_m, where two small semicircles with diameters of D_{m1} and D_{m2} are removed. Those parameters follow $D_{m1} = (D_m - w_1)/2$, $D_{m2} = (D_m - w_2)/2$, where w_1 and w_2 are the widths of two microstrip lines. Fig. 1(c) exhibits the circular coupling slot with diameter of D_s at mid ground layer. O_1, O_2, and O_3 are centers of three coupling slots, and parameter d is the distance between either two adjacent centers.

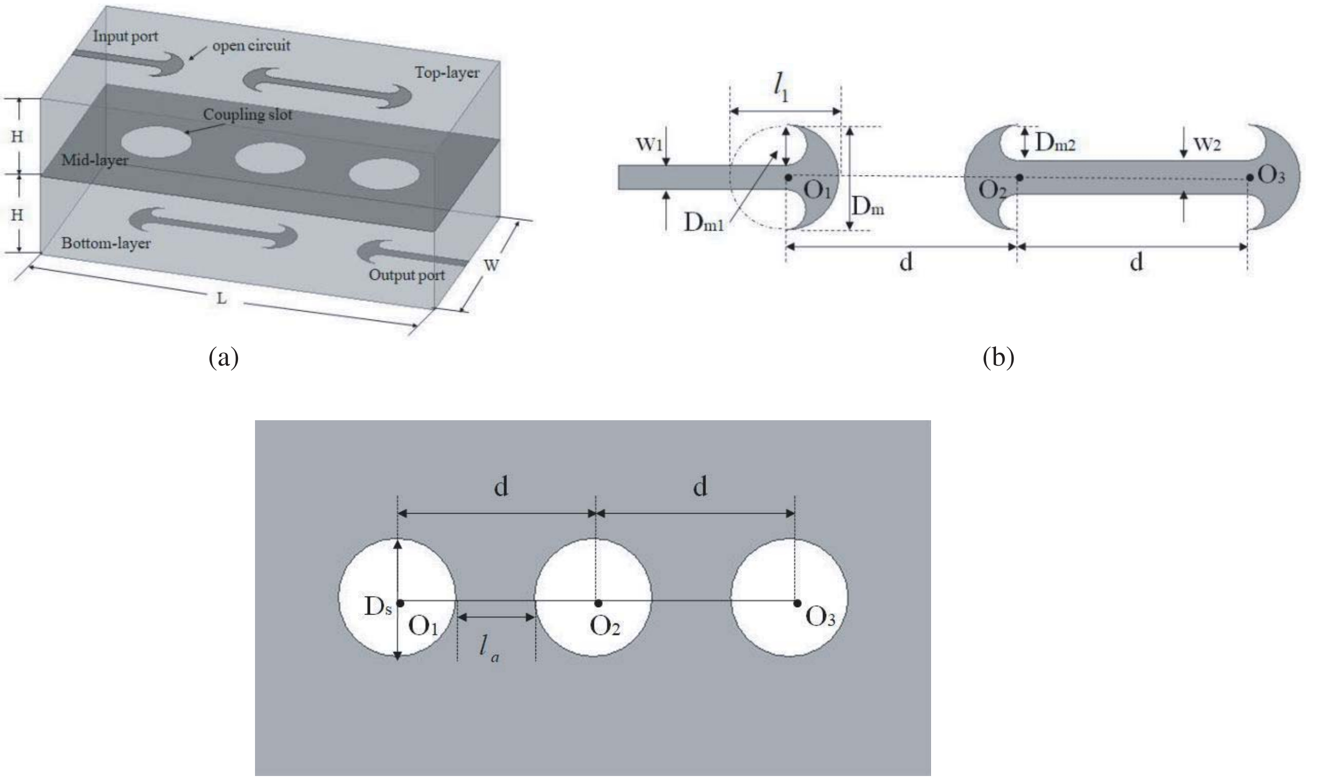

(a)

(b)

(c)

Figure 1. The structure and configuration of the proposed filter. (a) 3-D view. (b) The curved-T-shaped structure. (c) Coupling slot on the ground.

The edges of the curved T-shaped microstrip patches are open circuits, and the curved T-shaped microstrip patches at the top and bottom layers are coupled with the coupling slots at the mid common ground. The coupling unit belongs to a microstrip-slot broadside coupled structure [11], which could be equivalent to a two-port network, and its reflection coefficient S_{11} of the input and insertion loss S_{21}

of the output can be calculated as follows [9]:

$$S_{11} = \frac{1 - K^2\left[1 + \sin^2(\beta_{ef} l_1)\right]}{\left[\sqrt{1 - K^2}\cos(\beta_{ef} l_1) + j\sin(\beta_{ef} l_1)\right]^2} \tag{1}$$

$$S_{21} = \frac{j2K\sqrt{1 - K^2}\sin(\beta_{ef} l_1)}{\left[\sqrt{1 - K^2}\cos(\beta_{ef} l_1) + j\sin(\beta_{ef} l_1)\right]^2} \tag{2}$$

where K is the coupling coefficient of the curved T-shaped patches between top and bottom layers, β_{ef} the effective phase constant in the medium of the coupled structure, and the electrical length is $\beta_{ef} l_1 = \pi/2$. The length of coupling region l_1 is chosen by the one-quarter of guide wavelength at the center of the expected passband (6.85 GHz), here, $l_1 = D_m = 4.5\,\text{mm}$.

The schematic diagram of the signal flow between them when two coupling units are cascaded is shown in Fig. 2.

Figure 2. The schematic diagram of the signal flow between two coupling units.

Assume that a_i^j and b_i^j are the incident and reflected signals at the ith port of the jth section, respectively, and the microstrip lines are lossless and perfectly matched with the two coupling units. After two coupling units are cascaded, the return loss ($S_{11} = b_1^1/a_1^1$) and insertion loss ($S_{21} = b_2^2/a_1^1$) as a function of the S-parameters of its sections are equal to [9, 12]

$$S_{11} = S_{11}^1 + \frac{(S_{21}^1)^2 S_{11}^2 e^{-j2\beta_m l_a}}{1 - S_{11}^1 S_{11}^2 e^{-j\beta_m l_a}} \tag{3}$$

$$S_{21} = \frac{S_{21}^1 S_{21}^2 e^{-j\beta_m l_a}}{1 - S_{11}^1 S_{11}^2 e^{-j\beta_m l_a}} \tag{4}$$

where β_m is the phase constant of the microstrip line, and l_a is the physical length correspondingly, shown in Fig. 1(c), i.e., $l_a = d - D_s$. In order to minimize the unexpected mutual coupling between the top (or bottom) layers of those units, both input and output microstrip lines are $50\,\Omega$, thus $w_1 = w_2 = 1.15\,\text{mm}$. Fig. 3(a) shows the effect of l_a on the UWB filter's performance.

In fact, Eqs. (3) and (4) can be generalized for more (n) sections as follows

$$S_{11} = S_{11}^{\mathit{eff}(n-1)} + \frac{(S_{21}^{\mathit{eff}(n-1)})^2 S_{11}^n e^{-j2\beta_m l_a}}{1 - S_{11}^{\mathit{eff}(n-1)} S_{11}^n e^{-j\beta_m l_a}} \tag{5}$$

$$S_{21} = \frac{S_{21}^{\mathit{eff}(n-1)} S_{21}^n e^{-j\beta_m l_a}}{1 - S_{11}^{\mathit{eff}(n-1)} S_{11}^n e^{-j\beta_m l_a}} \tag{6}$$

where ($S_{11}^{\mathit{eff}(n-1)}$, $S_{21}^{\mathit{eff}(n-1)}$) and ($S_{11}^n$, S_{21}^n) are S-parameters of the first $(n-1)$ sections and the last section, respectively.

We can see from above analysis that f_0 is decided by l_1, and the best S-parameters after cascading coupling units are decided by l_a. Fig. 3(b) shows the performance of the UWB filter when taking $D_m = 4.5\,\text{mm}$, $l_a = 5.1\,\text{mm}$. The lower and upper frequencies are 4.4 GHz and 9.5 GHz. The insertion loss S_{21} and return loss S_{11} are better than $-3\,\text{dB}$ and $-15\,\text{dB}$, respectively. The passband has the 3 dB fractional bandwidth (FBW) of 88.2%, and the variation of group delay is 0.2 ns. There are five transmission poles generated within the passband, thus the coupling degree is enhanced.

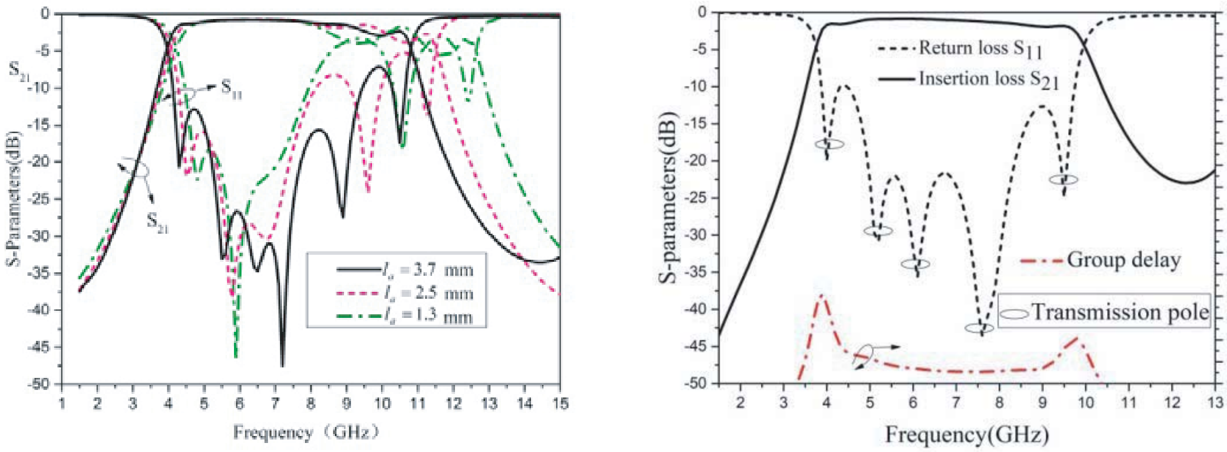

(a) (b)

Figure 3. The S parameters of UWB filter, where $D_m = 4.5\,\text{mm}$, $D_s = 5.3\,\text{mm}$, $w_1 = w_2 = 1.15\,\text{mm}$, $H = 0.508\,\text{mm}$, $L = 38\,\text{mm}$, $W = 15\,\text{mm}$. (a) The effect of l_a on the UWB filter's performance. (b) The S parameters of UWB when $l_a = 5.7\,\text{mm}$.

2.2. Implementation of Notched Filter

As depicted in Fig. 1(a), each coupling unit could be regarded as a parallel resonator consisting of an inductor L_P and a capacitor C_p. The whole circuit is formed by connecting three identical resonators in series, and the approximate equivalent circuit is shown in Fig. 4(a). Because the microstrips at the top and bottom layers have the common ground plane at the mid layer, C_g is the grounding capacitor shared by the adjacent resonators.

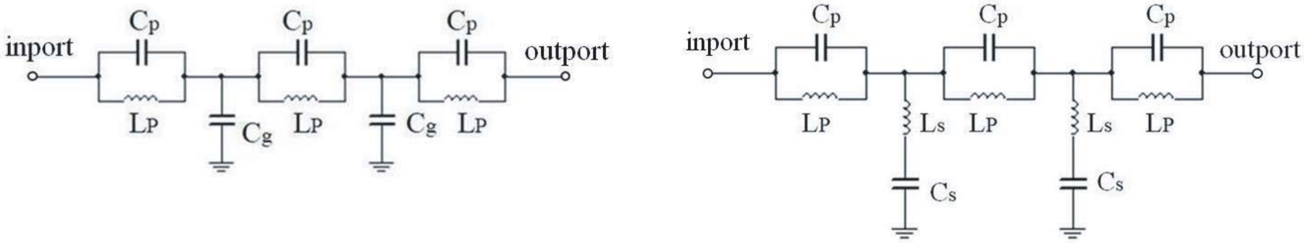

(a) (b)

Figure 4. Equivalent circuit of notched filter with curved-T-shaped. (a) The equivalent circuit of UWB filter. (b) The equivalent circuit of notched filter.

If a notched band is needed, we should introduce a stopband within the expected passband, thus the filter shown in Fig. 1(a) should be modified. Keep the other parameters of Fig. 3(b) unchanged, and let three coupling units be close enough to each other and partly overlapped, just as shown in Fig. 5, where $d = 4.12\,\text{mm}$, and l_2 is the physical length of the coupled slot. The S parameters are shown in Fig. 6, where f_n is the notch frequency; f_2 and f_1 are the upper and lower stopband frequencies of the notch, respectively; and the width of notched-band below $-10\,\text{dB}$ is 800 MHz. Two transmission poles in passband before and after the notch band enhance the coupling degree. Insertion loss S_{21} and return loss S_{11} are better than $-2\,\text{dB}$ and $-15\,\text{dB}$, and group delays are 0.08 ns and 0.12 ns. Compared with the UWB filter shown in Fig. 1, the whole passband moves to a lower band because the coupling length l_2 is much longer than l_1.

The equivalent circuit is shown in Fig. 4(b). Overlap of the curved T-shaped microstrip patches can be equivalent to grounding capacitors C_s and inductors L_s in series, thus a stopband circuit is

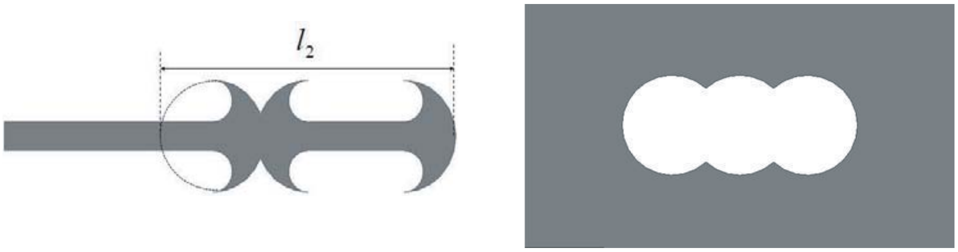

(a) (b)

Figure 5. The structure of the notched filter. (a) The curved-T-shaped structure of notched filter. (b) The structure of couple slot on the mid ground.

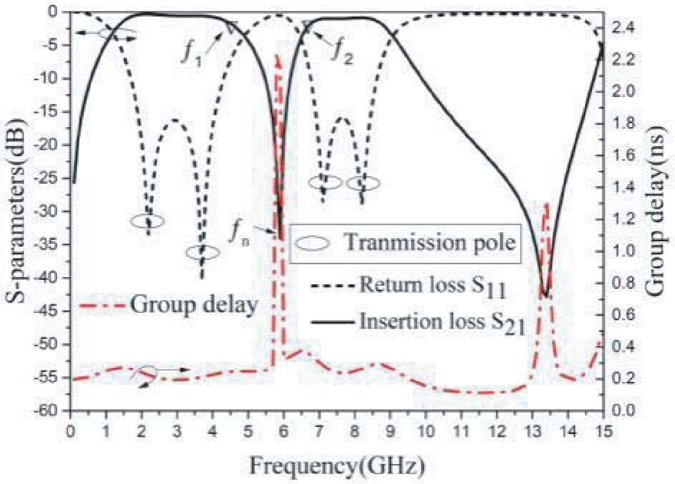

Figure 6. The S-parameters of the notched filter.

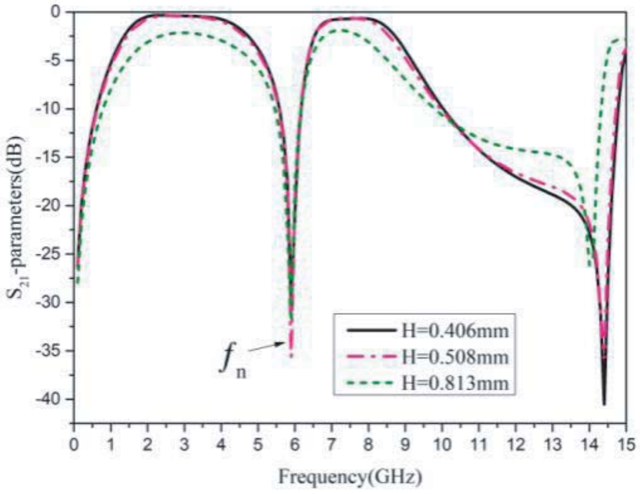

Figure 7. The effect of H on the S parameters.

formed between two resonators. This circuit can be regarded as that the grounding capacitance C_g is transformed to a bandstop circuit where C_s and L_s are connected in series. The relationships among C_s, L_s, and C_g are as follows [12]:

$$L_s = \frac{1}{2\pi \Delta C_g} \tag{7}$$

$$C_s = \frac{\Delta C_g}{2\pi f_n^2} \tag{8}$$

where the notched bandwidth $\Delta = f_2 - f_1$. According to Eqs. (7) and (8), C_g can be eliminated, and then f_n can be expressed as follows:

$$f_n = \frac{1}{2\pi \sqrt{C_s L_s}} \tag{9}$$

It is clear that f_n is independent of C_g, while C_g is related to the thickness of the substrate. Fig. 7 shows that, as H changes, f_n almost has no variation, and its value only depends on C_s and L_s.

2.3. Adjustment of the Notched Frequency

Based on the above analysis, it can be deduced that different values of C_s and L_s can affect f_n, while C_s and L_s can only be changed by adjusting the geometrical structure of the overlapped T-shaped patches. Three sets of values have been given to illustrate the influence of d and D_m in Fig. 8. Just as shown in Fig. 8(a), as d is increased, f_n moves from 6.5 GHz to 5.5 GHz, and Fig. 8(b) exhibits that f_n moves from 6 GHz to 5 GHz because of the increase of D_m, while the width of the notched bandwidth remains almost unchanged. The rules can be used to adjust the notched frequency to an interesting band and exclude other useless signals.

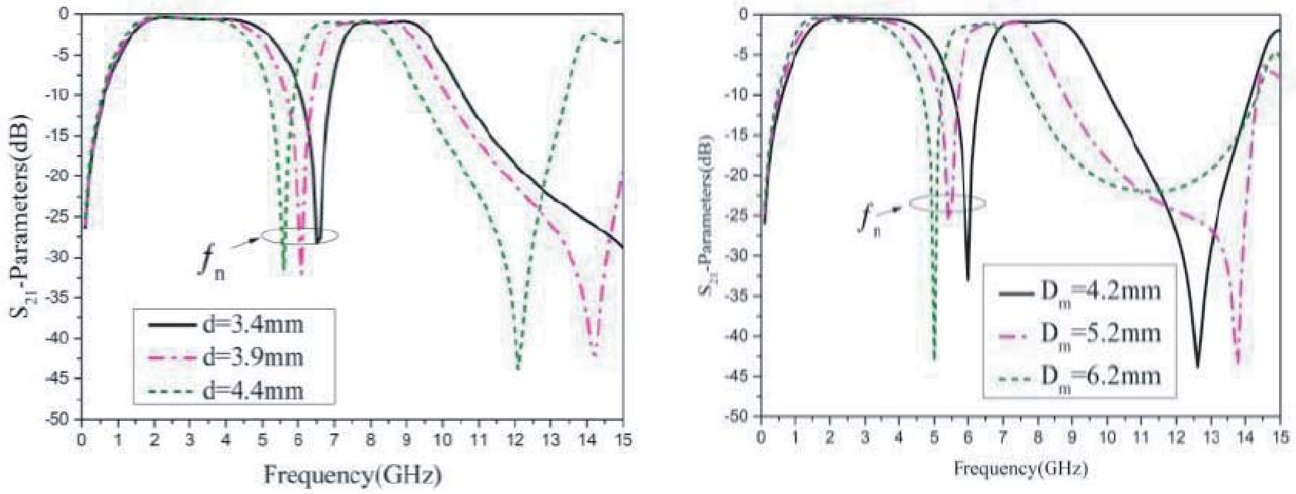

(a) (b)

Figure 8. The effect of D_m and d on the performance of the notched band with $D_s = 5.3$ mm, $w_1 = w_2 = 1.15$ mm, here, S_{21} is insertion loss. (a) The effect of D_m on the S parameters with $d = 4.12$ mm. (b) The effect of d on the S parameters with $D_m = 4.5$ mm.

3. IMPLEMENTATION AND RESULTS

A photograph of the fabricated filter is shown in Fig. 9(a), and Rogers 4003C is used as the dielectric substrate, with dielectric constant $\varepsilon_r = 3.55$, loss tangent $\delta = 0.0029$, and thickness 0.508 mm. The physical circuit has considered the WLAN signals of 5.8 GHz, here taking $w_1 = 1.15$ mm, $w_2 = 1.15$ mm, $D_m = 4.22$ mm, $d = 4.12$ mm, $D_s = 5.02$ mm. Simulated and measured results of S parameters are

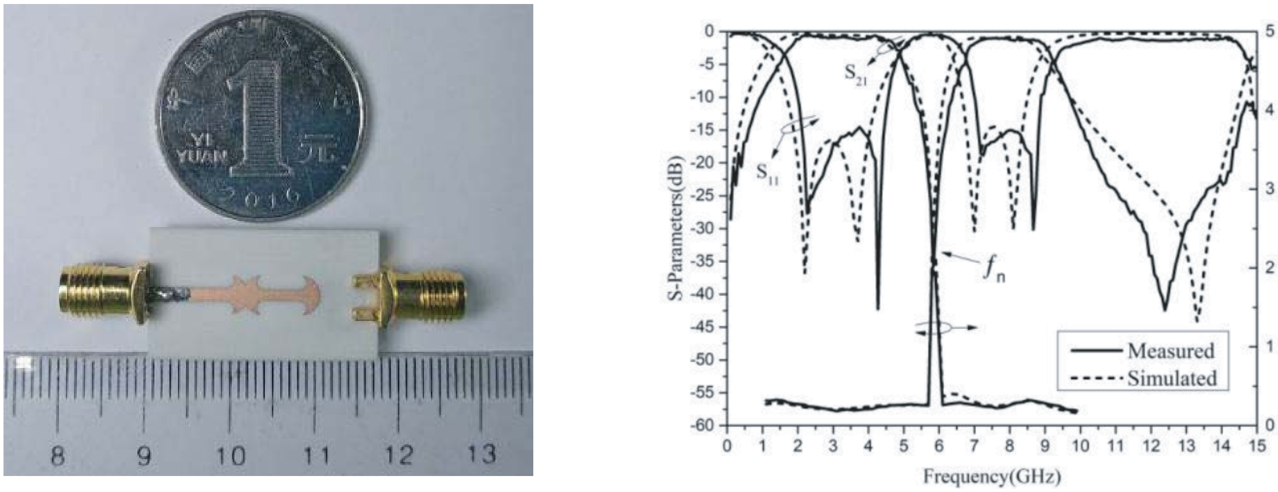

(a) (b)

Figure 9. Photograph of the notched filter and experimental and simulated S-parameter results. (a) The photograph of the band notched filter. (b) Experimental and simulated S-parameter results.

shown in Fig. 9(b). The notched frequency is at 5.8 GHz, and the width of notched-band below -10 dB is 1.1 GHz (5.3–6.4 GHz). The in-band group delays before and after the notched band are 0.08 ns and 0.12 ns. Measured and simulated results have an error of approximately 0.2 GHz within the passband due to insufficient precision in circuit fabrication. The overall size of the circuit is $L \times W = 26.7\,\text{mm} \times 15\,\text{mm}$.

4. CONCLUSION

In this paper, a wideband filter with notched characteristics is proposed, which is composed of curved T-shaped microstrip patches. The feasibility is verified by fabricated production. The notched band can be flexibly adjusted by regulating the length of the coupling regions. The filter has a compact size and excellent performance.

ACKNOWLEDGMENT

This work is supported by the Natural Science Foundation of Tianjin, China (18JCYBJC16400), Graduate Innovation Fundation of Tianjin University of Technology and Education in 2017, China (YC18-34) and Tianjin Research Program of Application Foundation and Advanced Technology (14JCQNJC01100).

REFERENCES

1. Federal Communications Commission, "Revision of Part 15 of the Commission's rules regarding ultra-wideband transmission systems," Tech. Rep., ET-Docket 98–153, FCC02–48, Apr. 2002.
2. Zhu, L., S. Sun, and W. Menzel, "Ultra-wideband (UWB) bandpass filters using multiple-mode resonator," *IEEE Microwave and Wireless Components Letters*, Vol. 15, No. 11, 796–798, 2005.
3. Mokhtaari, M., J. Bornemann, and S. Amari, "A modified design approach for compact ultra-wideband microstrip filters," *International Journal of RF and Microwave Computer-Aided Engineering*, Vol. 20, No. 1, 66–75, 2010.
4. Hao, S. and T. Jiang, "A compact ultra-wideband band-pass filter integrated with dual tunable notch bands," *2016 Progress In Electromagnetic Research Symposium (PIERS)*, 3492–3494, Shanghai, China, Aug. 8–11, 2016.

5. Sarkar, P., R. Ghatak, M. Pal, D. R. Poddar, et al., "Compact UWB bandpass filter with dual notch bands using open circuited stubs," *IEEE Microwave & Wireless Components Letters*, Vol. 22, No. 9, 453–455, 2012.
6. Luo, X., et al., "Compact UWB bandpass filter with ultra narrow notched band," *IEEE Microwave & Wireless Components Letters*, Vol. 20, No. 3, 145–147, 2010.
7. Kumar, S., R. D. Gupta, and M. S. Parihar, "Multiple band notched filter using C-shaped and E-shaped resonator for UWB applications," *IEEE Microwave & Wireless Components Letters*, Vol. 26, No. 5, 340–342, 2016.
8. Abbosh, A. and M. Bialkowski, "Design of compact directional couplers for UWB applications," *IEEE Trans. Microw. Theory Tech.*, Vol. 55, No. 2, 189–194, 2007.
9. Abbosh, A., "Planar bandpass filters for ultra wideband applications," *IEEE Trans. Microw. Theory Tech.*, Vol. 55, No. 10, 2262–2269, 2007.
10. Abbosh, A., M. Bialkowski, and D. Thiel, "Ultra wideband bandpass filter using microstrip-slot couplers combined with dumbbell slots and H-shaped stubs," *Proc. Asia-Pacific Microw. Conf.*, 909–912, Singapore, Dec. 7–10, 2009.
11. Mongia, R., I. Bahl, and P. Bhartia, *RF and Microwave Coupled-line Circuits*, Vol. 109, 117–119, Artech House, Norwood, MA, 1999.
12. Pozar, D., *Microwave Engineering*, 3rd edition, Wiley, New York, 2005.